

FULL PAPER

Magnetically recoverable copper nanorods and their catalytic activity in Ullmann cross-coupling reaction

Maryam Rajabzadeh¹ | Hossein Eshghi¹ | Reza Khalifeh² | Mehdi Bakavoli¹

¹Department of Chemistry, Faculty of Sciences, Ferdowsi University of Mashhad, Mashhad 91775-1436, Iran

²Department of Chemistry, Shiraz University of Technology, 71555-313 Shiraz, Iran

Correspondence

Hossein Eshghi, Department of Chemistry, Faculty of Sciences, Ferdowsi University of Mashhad, Mashhad 9177948974, Iran.
Email: heshghi@um.ac.ir

A novel polydentate ligand supported on Fe₃O₄@SiO₂ was designed and demonstrated for the synthesis of Cu nanorods. The Fe₃O₄@SiO₂/EP.EN.EG@Cu was characterized using X-ray diffraction, thermogravimetric analysis, transmission electron microscopy, energy-dispersive X-ray spectroscopy and vibrating sample magnetometry. The Fe₃O₄@SiO₂/EP.EN.EG@Cu showed excellent catalytic efficiency for the cross-coupling reaction of nitrogen-containing heterocycles with aryl halides. The catalyst could be effectively separated from the reaction mixture by simply applying an external magnetic field and reused at least five times without loss of activity.

KEYWORDS

Cu nanorods, Fe₃O₄@SiO₂/EP.EN.EG, nanocatalyst, Ullmann reaction

1 | INTRODUCTION

The C–N bond formation reaction is one of the most important reactions and has proved to be challenging in industrial and medicinal settings.^[1] Ullmann and Goldberg first developed the introduction of an amino group via copper-catalysed cross-coupling reactions (stoichiometric amounts of copper salts were used to activate aryl halides) that have been extensively investigated by many researchers.^[2,3] Many efforts have been directed at achieving mild and inexpensive reaction conditions for C–N bond formation reactions. Most of these processes are carried out in the presence of metal complexes. Numerous copper-containing complexes with new ligands have been designed which allow the formation of important products via C–N bond cross-coupling.^[4–6] A complex of CuBr with *N,N'*-dimethylethylenediamine (DMEDA) was reported for the cyclization of *ortho*-gem-dibromovinyl anilines and benzoyl chloride.^[7] Also, complexes of copper salts and various ligands such as 2-acetylcyclohexanone,^[8] 2,2'-bipyridine,^[9] 2-(2,6-dimethylphenylamino)-2-oxoacetic acid^[10] and DMEDA^[11] were investigated for C–N bond cross-coupling reactions. The catalytic reactions occur on the surface of metal nanoparticles (NPs), and are mainly dependent on their size and shape.^[12] Design of metal NPs with various sizes and shapes is a major research area due to the fact that metals

have different properties compared to their bulk counterparts.^[13–17] Recently, the synthesis of metal nanorods, especially with metallic copper, of various sizes in high yield and of monodispersity has been developed.^[18–20] But only a few papers have been published related to their applications in organic syntheses. Various methods such as the thermal, photochemical and sonochemical reduction of Cu(II) complexes for the synthesis of Cu NPs of various shapes have been reported.^[21,22] Anionic surfactants such as C_{11–17}COOH and sodium dodecylsulfate were used for stabilizing Cu(II) ions through electrostatic interactions and further *in situ* reduction promotes the formation of Cu NPs of different sizes and shapes.^[23] Bhaumik and co-workers reported a method for the preparation of Cu nanospheres and nanorods via a hydrothermal process utilizing the templating property of a fatty acid with or without the addition of ethylenediamine.^[24] Also, dispersion of NPs onto supports for increasing availability and avoiding of NP agglomeration is effective. Furthermore, surface modification with various functional groups such as –NH_n and –OH groups via strong interaction between Cu NPs affects the catalytic properties. Fe₃O₄ magnetic NPs have been employed as an excellent choice for catalyst supports, due to their easy recovery using an external magnetic field. Their insoluble and superparamagnetic natures make it possible to realize various reactions and reduce capital and operational costs.^[25,26]

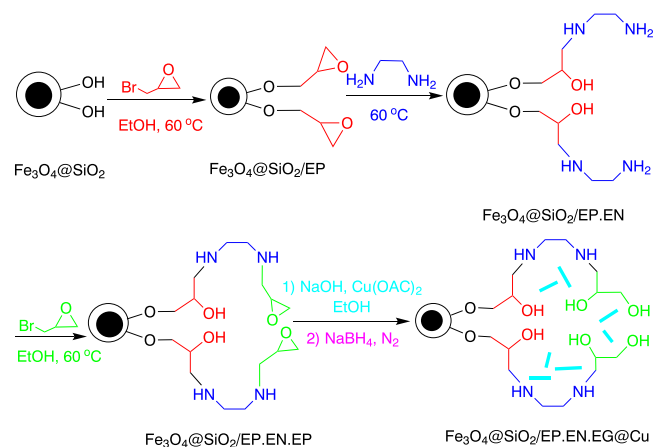
In this article, we demonstrate the efficiency of a newly designed polydentate ligand (EP.EN.EG) for the synthesis of Cu nanorods. In fact, our designed ligand can control the shape of Cu NPs. So that, without any stabilizing agent, this ligand can act as a templating agent. The efficiency of $\text{Fe}_3\text{O}_4@SiO_2@EP.EN.EG@Cu$ in the Ullmann reaction was evaluated.

2 | RESULTS AND DISCUSSION

The Fe_3O_4 magnetic NPs were prepared via a co-precipitation method and then were coated with silica via the Stober method.^[27] The $\text{Fe}_3\text{O}_4@SiO_2@EP.EN.EP$ was prepared in a three-step procedure.^[28] The Cu nanorods were then obtained by mixing Cu(II) acetate and $\text{Fe}_3\text{O}_4@SiO_2@EP.EN.EP$ in a refluxing ethanol solution in the presence of NaOH in 12 h. Finally, NaBH_4 was added to mixture reaction for synthesis of $\text{Fe}_3\text{O}_4@SiO_2/EP.EN.EG@Cu$ (Scheme 1). This nanocatalyst was characterized using X-ray diffraction (XRD), thermogravimetric analysis (TGA), transmission electron microscopy (TEM), energy-dispersive X-ray spectroscopy (EDS) and vibrating sample magnetometry (VSM).

The crystal structures of Fe_3O_4 , $\text{Fe}_3\text{O}_4@SiO_2$ and $\text{Fe}_3\text{O}_4@SiO_2/EP.EN.EG@Cu$ were identified using XRD characterization (Figure 1). The peaks located at 30.31° , 35.64° , 43.31° , 53.86° , 57.24° and 62.83° could be attributed to (220), (311), (400), (422), (511) and (440) crystal planes, which, as observed, were in agreement with the standard data for Fe_3O_4 (cubic phase) (Figure 1a). The broad peak observed at $2\theta = 23^\circ$ could be allocated to the amorphous silica shell (Figure 1b). As the XRD pattern of $\text{Fe}_3\text{O}_4@SiO_2/EP.EN.EG@Cu$ shows (Figure 1c), there was a decline in peak intensity compared to that of $\text{Fe}_3\text{O}_4@SiO_2$ which generally indicates retained crystal structure of the Fe_3O_4 core after modification. Additionally, new peaks were observed at $2\theta = 51.52^\circ$ and 74.24° which could be attributed to the Cu nanorods in the catalysis matrix.

The thermal behaviour of organic functional groups anchored on $\text{Fe}_3\text{O}_4@SiO_2$ was investigated using TGA



SCHEME 1 Synthetic route to $\text{Fe}_3\text{O}_4@SiO_2/EP.EN.EG@Cu$

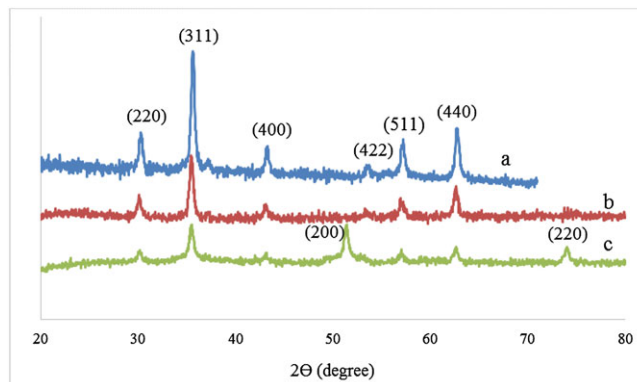


FIGURE 1 XRD patterns: (a) Fe_3O_4 ; (b) $\text{Fe}_3\text{O}_4@SiO_2$; (c) $\text{Fe}_3\text{O}_4@SiO_2/EP.EN.EG@Cu$

(Figure 2). A significant weight decrease observed around 100°C was due to desorption of water molecules on the support. A weight loss of 13% appearing at $190\text{--}600^\circ\text{C}$ was a result of decomposition of organic groups loaded on the $\text{Fe}_3\text{O}_4@SiO_2$ surface. TGA curves confirm that the amount of the organic part grafted on the surface of the catalyst was about 0.6 mmol g^{-1} .

In addition, TEM images were used to examine the morphology and size of $\text{Fe}_3\text{O}_4@SiO_2$ and $\text{Fe}_3\text{O}_4@SiO_2/EP.EN.EG@Cu$ (Figure 3). It was observed that $\text{Fe}_3\text{O}_4@SiO_2$ consisted of spherical structures and that the average size of the magnetic NPs was about 20 nm (Figure 3a). Figure 3(b) shows a TEM image of the $\text{Fe}_3\text{O}_4@SiO_2/EP.EN.EG@Cu$. The Cu nanorods with an average size of about 10 nm are uniformly distributed on the surfaces of the catalyst. Moreover, the presence of Cu, Fe and Si was confirmed through the EDS spectrum (Figure 4). The amount of Cu loaded on the magnetic nanoparticles was estimated to be 2.59 mmol g^{-1} based on inductively coupled plasma atomic emission spectroscopy (ICP) results.

The magnetic responsiveness plays a very significant role for magnetic materials. Thus, the magnetic properties of Fe_3O_4 , $\text{Fe}_3\text{O}_4@SiO_2$ and $\text{Fe}_3\text{O}_4@SiO_2/EP.EN.EG@Cu$ were analysed using VSM at room temperature (Figure 5). The

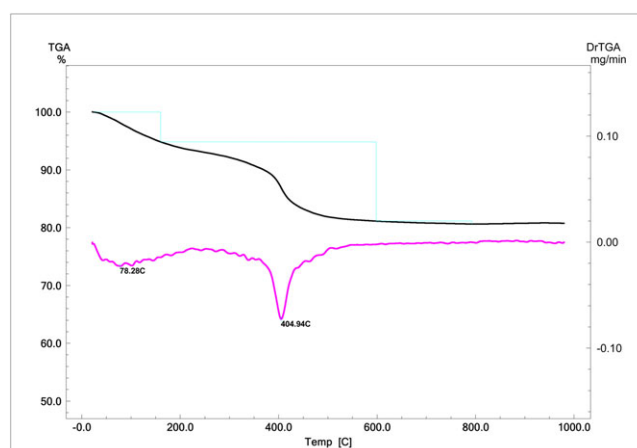


FIGURE 2 TGA thermogram of $\text{Fe}_3\text{O}_4@SiO_2/EP.EN.EG$

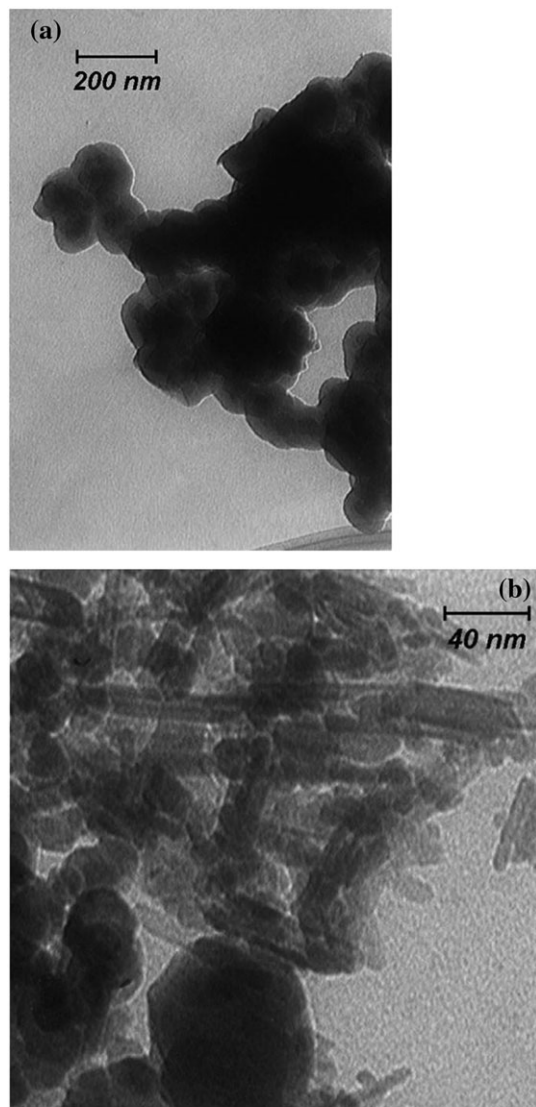


FIGURE 3 TEM images: (a) $\text{Fe}_3\text{O}_4@SiO_2$; (b) $\text{Fe}_3\text{O}_4@SiO_2/EP.EN. EG@Cu$

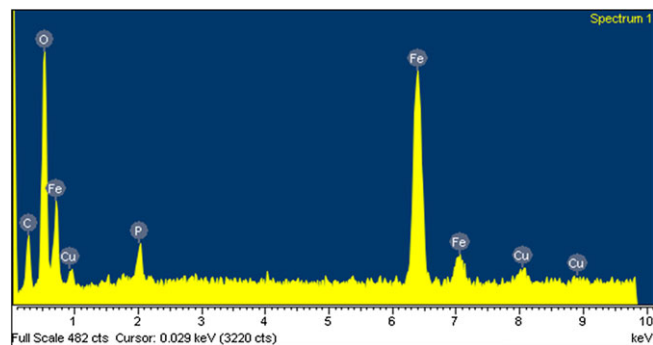


FIGURE 4 EDS spectrum of $\text{Fe}_3\text{O}_4@SiO_2/EP.EN. EG@Cu$

saturation magnetization (M_s) values of these magnetic samples are 63.6, 37.8 and 29.4 emu g^{-1} , respectively. The results showed that M_s values for $\text{Fe}_3\text{O}_4@SiO_2$ and $\text{Fe}_3\text{O}_4@SiO_2/EP.EN. EG@Cu$ have decreased, compared to

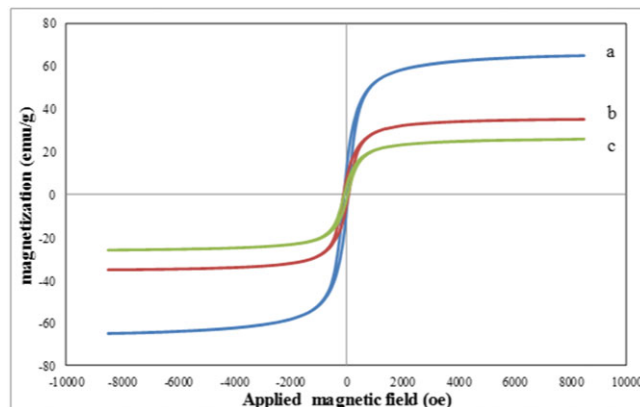
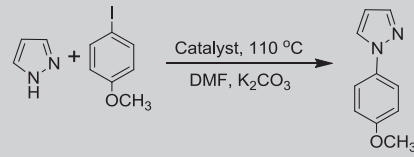


FIGURE 5 Magnetization curves: (a) Fe_3O_4 ; (b) $\text{Fe}_3\text{O}_4@SiO_2$; (c) $\text{Fe}_3\text{O}_4@SiO_2/EP.EN. EG@Cu$

the uncoated Fe_3O_4 . These decreases occur as a result of the increase in mass and size after the SiO_2 shell coating and the anchoring of Cu nanorods. Also, there was found no noticeable remanence or coercivity in the magnetization curves, showing superparamagnetic character. Thus, an external magnet can readily separate the new magnetic material.

One of the goals of the research reported here was to estimate the activity of $\text{Fe}_3\text{O}_4@SiO_2/EP.EN. EG@Cu$ as a catalyst for the cross-coupling reactions of N-heterocyclic compounds with aryl halides. The reaction of 1*H*-pyrazole and *p*-methoxyanisole in the presence of $\text{Fe}_3\text{O}_4@SiO_2/EP.EN. EG@Cu$ was chosen as a model and its behaviour was studied under a variety of conditions via TLC and NMR spectroscopy (Table 1). Initially, the effect of solvent was studied based on isolated yield. These results indicated that dimethylformamide (DMF) was the best choice for this reaction (Table 1, entry 7), while other solvents such as dimethylsulfoxide (DMSO), water, toluene and CH_3CN gave lower yields (Table 1, entries 1–4). In order to determine the best base, the model reaction was carried out in the presence of K_2CO_3 , NaHCO_3 and KOH (Table 1, entries 7, 8 and 9). Among them, K_2CO_3 was found to be highly efficient for the cross-coupling reaction. In addition, temperature is also important for the progress of the reaction. At temperatures below 110 $^\circ\text{C}$, the desired product was detected in lower yield (Table 1, entries 5 and 6). The influence of the amount of catalyst was evaluated using the model reaction. No reaction was observed in the absence of the catalyst (Table 1, entry 10). The best result was achieved when the amount of catalyst was increased from 1.3 to 8 mol% (Table 1, entries 10–13).

With these optimal conditions, we investigated the coupling of nitrogen-containing heterocycles with a variety of aryl halides bearing either an electron-donating group or an electron-withdrawing group (Table 2). We found that the arylation of pyrazole, benzimidazole and triazole with aryl iodide provided higher yields in shorter reaction times than with aryl bromide (Table 2, entries 1, 2, 9, 10, 14 and 15). In the case of 1-iodo-4-bromobenzene, substitution occurs in C–I bond as a main product, but C–Br product

TABLE 1 Optimization of reaction conditions for *N*-arylation of 1*H*-pyrazole^a


Entry	Base	Solvent	Amount of catalyst (mol%)	Yield (%)
1	K ₂ CO ₃	H ₂ O	8	20
2	K ₂ CO ₃	CH ₃ CN	8	60
3	K ₂ CO ₃	Toluene	8	40
4	K ₂ CO ₃	DMSO	8	60
5 ^b	K ₂ CO ₃	DMF	8	60
6 ^c	K ₂ CO ₃	DMF	8	30
7	K ₂ CO ₃	DMF	8	98
8	NaHCO ₃	DMF	8	Trace
9	KOH	DMF	8	50
10	K ₂ CO ₃	DMF	—	0
11	K ₂ CO ₃	DMF	1.3	30
12	K ₂ CO ₃	DMF	2	50
13	K ₂ CO ₃	DMF	2.6	75

^aReaction conditions: *p*-methoxyiodobenzene (1 mmol), 1*H*-pyrazole (1.2 mmol), catalyst (8 mol%), base (2 mmol) and solvent (5 ml) at 110 °C.

^bReaction carried out at 90 °C.

^cReaction carried out at 70 °C.

substitution was also observed (Table 2, entries 12 and 16). However, for 2-iodo-5-bromopyridine, *N*-arylation occurs selectively only at C-5 (Table 2, entries 4 and 13). Compared with electron-donating groups on aryl iodide or

benzimidazole (Table 2, entries 1 and 5), electron-withdrawing groups (Table 2, entries 3, 6 and 7) led to higher yields. In addition, the reactions of heterocyclic compounds such as pyrazole, triazole, indole and 1*H*-benzo[*d*] [1-3]triazole with aryl iodide were examined. The results show excellent yields of the corresponding products (Table 2, entries 8, 9, 11, 14 and 17).

The reusability of the catalyst was tested in the model reaction (Table 3). After the completion of the reaction, the catalyst was separated from the product using an external magnet. To remove all organic compounds, the catalyst was washed with ethanol, dried at 50 °C under vacuum and reused for five times without a significant decline in its catalytic activity.

The Fe₃O₄@SiO₂/EP.EN.EG@Cu recovered after the fifth run was characterized using TEM and ICP. As shown in Figure 6, the TEM image of the reused catalyst did not portray a significant change compared to the fresh catalyst. The amount of Cu loaded in the catalyst used for five times was determined using elemental analysis (ICP) as 1.82 mmol g⁻¹. Therefore, these results indicated that the morphology and

TABLE 3 Reusability of catalyst for *N*-arylation of nitrogen-containing heterocycles

Run	Yield (%)
1	98
2	98
3	95
4	90
5	90

TABLE 2 Fe₃O₄@SiO₂/EP.EN.EG@Cu-catalysed *N*-arylation of various nitrogen-containing heterocycles with aryl halides^a

Entry	Aryl halide	Heterocycle	Time (h)	Yield (%)
1	<i>p</i> -Methoxyiodobenzene	Benzimidazole	18	85
2	<i>p</i> -Methoxybromobenzene	Benzimidazole	20	70
3	1-Iodo-2-methyl-4-nitrobenzene	Benzimidazole	16	90
4	5-Bromo-2-iodopyridine	Benzimidazole	14	95
5	<i>p</i> -Methoxyiodobenzene	2-Methyl-1 <i>H</i> -benzimidazole	20	80
6	<i>p</i> -Methoxyiodobenzene	5-Nitro-1 <i>H</i> -benzimidazole	16	90
7	1-Iodo-4-nitrobenzene	5-Nitro-1 <i>H</i> -benzimidazole	16	95
8	<i>p</i> -Methoxyiodobenzene	Indole	18	90
9	<i>p</i> -Methoxyiodobenzene	1 <i>H</i> -pyrazole	12	98
10	<i>p</i> -Methoxybromobenzene	1 <i>H</i> -pyrazole	18	85
11	1-Iodo-2-methyl-4-nitrobenzene	1 <i>H</i> -pyrazole	16	98
12	1-Bromo-4-iodobenzene	1 <i>H</i> -pyrazole	12	80
13	5-Bromo-2-iodopyridine	1 <i>H</i> -pyrazole	14	95
14	<i>p</i> -Methoxyiodobenzene	1 <i>H</i> -1,2,4-triazole	14	98
15	<i>p</i> -Methoxybromobenzene	1 <i>H</i> -1,2,4-triazole	16	90
16	1-Bromo-4-iodobenzene	1 <i>H</i> -1,2,4-triazole	12	85
17	<i>p</i> -Methoxyiodobenzene	1 <i>H</i> -benzo[<i>d</i>] [1-3]triazole	16	90

^aAryl halides (1 mmol), nitrogen-containing heterocycles (1.2 mmol), catalyst (8 mol%) and K₂CO₃ (2 mmol) in DMF (5 ml) as solvent at 110 °C.

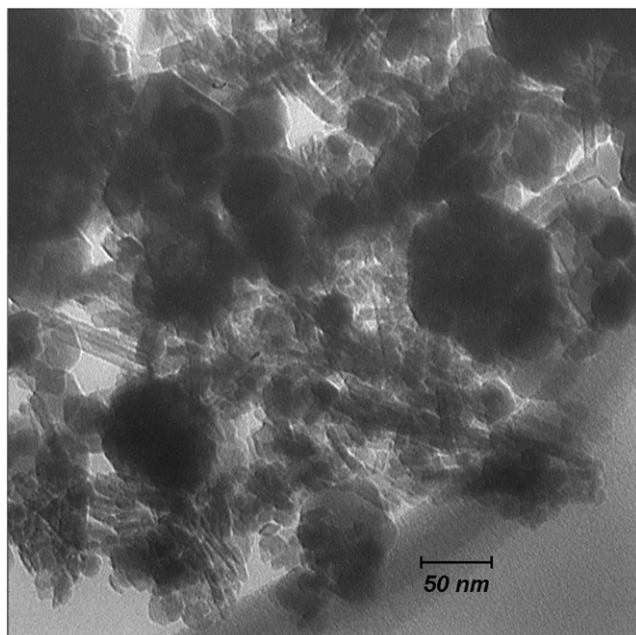


FIGURE 6 TEM image of $\text{Fe}_3\text{O}_4@SiO_2/EP.EN.EG@Cu$ after five recycles

structure of the catalyst were the same, and the leaching of Cu was low, after the fifth run.

The catalytic activity of $\text{Fe}_3\text{O}_4@SiO_2/EP.EN.EG@Cu$ was compared with that of systems previously reported (Table 4) as applied in the cross-coupling reactions of nitrogen-containing heterocycles with aryl halides. It is clear that $\text{Fe}_3\text{O}_4@SiO_2/EP.EN.EG@Cu$ is the most effective catalyst for *N*-arylation of nitrogen-containing heterocycles, leading to the formation of products in high yield.

3 | EXPERIMENTAL

Mass spectra were recorded with a 5973 Network mass selective detector. ^1H NMR spectra were recorded with a Bruker AC 300 MHz instrument in $\text{DMSO}-d_6$ or CDCl_3 . TGA was performed with a Shimadzu TG-50 thermogravimetric analyser. TEM images were acquired using a Leo 912 AB 120 kV TEM microscope (Zeiss, Germany). Elemental compositions were determined using an EDS instrument with 133 eV resolution (7353, Oxford, UK). ICP analysis was conducted obtained using a Varian VISTAPRO CCD (Australia). XRD patterns were collected using a Bruker D4

X-ray diffractometer with Ni-filtered $\text{Cu K}\alpha$ radiation (40 kV, 30 mA).

3.1 | General procedure for preparation of $\text{Fe}_3\text{O}_4@SiO_2/EP.EN.EP$

In the first step, the synthesis of core-shell $\text{Fe}_3\text{O}_4@SiO_2$ microspheres was carried out using the Stober sol-gel method.^[27] In the second step, a mixture of epibromohydrin (10 mmol, 1.36 g) and $\text{Fe}_3\text{O}_4@SiO_2$ (0.5 g) in ethanol (3 ml) was stirred for 5 h at 60 °C. $\text{Fe}_3\text{O}_4@SiO_2/EP$ was separated using an external magnet, washed with ethanol and dried at 80 °C. Ethylenediamine (5 ml) was added to dried $\text{Fe}_3\text{O}_4@SiO_2/EP$ and stirred at 60 °C. After 24 h, the solid was collected, washed with methanol and dried at 80 °C to afford $\text{Fe}_3\text{O}_4@SiO_2/EP.EN$. Then the dried precipitate was added to a solution of epibromohydrin (10 mmol, 1.36 g) in ethanol (3 ml) at 60 °C for 5 h. Finally, the product was separated using an external magnet, washed with methanol and dried at 80 °C.^[28]

3.2 | General procedure for preparation of Cu nanorods loaded on magnetic core ($\text{Fe}_3\text{O}_4@SiO_2/EP.EN.EG@Cu$)

$\text{Cu}(\text{OAc})_2$ (0.25 g) and $\text{Fe}_3\text{O}_4@SiO_2/EP.EN.EP$ (0.5 g) were dissolved in absolute ethanol (5 ml) and then NaOH solution was added to mixture under vigorous stirring until a pH of 12–13 was achieved. After reaction under reflux for 12 h, a solution of sodium borohydride (10 ml, 0.15 mol l^{-1}) was added dropwise to the mixture and stirred under nitrogen atmosphere for 2 h. The product ($\text{Fe}_3\text{O}_4@SiO_2/EP.EN.EG@Cu$) was collected using a magnet. Washed with methanol and dried under vacuum at room temperature for 8 h.

3.3 | General procedure for *n*-arylation of *n*-heterocyclic compounds with aryl halides

$\text{Fe}_3\text{O}_4@SiO_2/EP.EN.EG@Cu$ (0.03 g) as a catalyst was added to a mixture of aryl halide (1 mmol), *N*-heterocyclic compound (1.2 mmol) and K_2CO_3 (2 mmol) in DMF at 110 °C. After completion of the reaction, the catalyst was separated using an external magnet and washed with ethyl acetate. The product was extracted with ethyl acetate and purified using column chromatography with hexane–ethyl acetate as a solvent system.

TABLE 4 Comparison of various catalysts for *N*-arylation of 1*H*-pyrazole

Entry	Catalyst	Temp (°C)	Time (h)	Yield (%)	Ref.
1	$\text{Cu}(\text{OAc})_2 \cdot \text{H}_2\text{O}$	110	24	95	[29]
2	Cu_2O	80	18	95	[30]
3	Copper decorated OMMT	130	10	70	[31]
4	$[\text{Cu}(\text{Im}1_2)_2]\text{CuCl}_2$	80	12	75	[32]
5	$\text{Fe}_3\text{O}_4@SiO_2/EP.EN.EG@Cu$	110	12	95	This work

3.3.1 | 1-(4-Methoxyphenyl)-1H-benzo[d]imidazole (Table 2, entry 1)

¹H NMR (DMSO, 300 MHz, δ , ppm): 3.85 (s, 3H), 7.17 (d, 2H, $J = 8.7$ Hz), 7.27–7.79 (m, 4H), 7.59 (d, 2H, $J = 9$ Hz), 8.47 (s, 1H). ¹³C NMR (75 MHz, DMSO, δ , ppm): 56.00, 110.92, 115.60, 120.31, 122.69, 123.75, 125.90, 129.26, 134.07, 143.98, 159.16. MS (EI): m/z (%) 224 [M^+].

3.3.2 | 1-(2-Methyl-4-nitrophenyl)-1H-benzo[d]imidazole (Table 2, entry 3)

¹H NMR (CDCl₃, 300 MHz, δ , ppm): 2.30 (s, 3H), 7.16 (dd, 1H, $J^1 = 6.6$ Hz, $J^2 = 1.5$ Hz), 7.34–7.43 (m, 2H), 7.55 (d, 1H, $J = 8.7$ Hz), 7.94 (d.d, 1H, $J^1 = 6$ Hz, $J^2 = 2.1$ Hz), 8.21 (s, 1H), 8.27 (d.d, 1H, $J^1 = 8.4$ Hz, $J^2 = 2.4$ Hz), 8.36 (d, 1H, $J = 2.1$ Hz). ¹³C NMR (75 MHz, CDCl₃, δ , ppm): 18.17, 110.16, 120.90, 122.54, 123.23, 124.25, 126.78, 128.51, 134.04, 137.10, 140.34, 142.11, 143.48, 147.71. MS (EI): m/z (%) 253 [M^+].

3.3.3 | 1-(6-Iodopyridin-3-yl)-1H-benzo[d]imidazole (Table 2, entry 4)

¹H NMR (CDCl₃, 300 MHz, δ , ppm): 7.34–7.39 (m, 2H), 7.76 (d, 1H, $J = 6.6$ Hz), 7.96 (d, 1H, $J = 8.7$ Hz), 8.26–8.33 (m, 1H), 8.76 (d, 1H, $J = 2.4$ Hz), 8.85 (d, 1H, $J = 1.8$ Hz), 8.98 (s, 1H). ¹³C NMR (75 MHz, CDCl₃, δ , ppm): 113.51, 115.72, 119.36, 123.52, 131.14, 141.39, 143.63, 146.69, 148.22, 148.87, 153.84. MS (EI): m/z (%) 320 [M^+].

3.3.4 | 1-(4-Methoxyphenyl)-2-methyl-1H-benzo[d]imidazole (Table 2, entry 5)

¹H NMR (DMSO, 300 MHz, δ , ppm): 2.51 (s, 3H), 3.93 (s, 3H), 7.09–7.31 (m, 7H), 7.65 (d, 1H, $J = 7.2$ Hz). ¹³C NMR (75 MHz, DMSO, δ , ppm): 14.33, 55.63, 109.92, 115.05, 118.92, 122.35, 128.34, 128.66, 136.84, 142.50, 151.95, 159.75. MS (EI): m/z (%) 238 [M^+].

3.3.5 | 1-(4-Methoxyphenyl)-5-nitro-1H-benzo[d]imidazole (Table 2, entry 6)

¹H NMR (CDCl₃, 300 MHz, δ , ppm): 3.88 (s, 3H), 7.23–8.87 (m, 8H). MS (EI): m/z (%) 269 [M^+].

3.3.6 | 5-Nitro-1-(4-nitrophenyl)-1H-benzo[d]imidazole (Table 2, entry 7)

¹H NMR (CDCl₃, 300 MHz, δ , ppm): 7.68 (1H, d, $J = 9$ Hz), 7.79 (d, 2H, $J = 9$ Hz), 8.37 (dd, 1H, $J^1 = 9$ Hz, $J^2 = 2.1$ Hz), 8.38 (s, 1H), 8.56 (d, 2H, $J = 9$ Hz), 8.86 (d, 1H, $J = 2.1$ Hz). ¹³C NMR (75 MHz, CDCl₃, δ , ppm): 110.41, 117.86, 120.24, 124.42, 126.13, 136.89, 140.46, 143.91, 144.80, 147.44. MS (EI): m/z (%) 284 [M^+].

3.3.7 | 1-(4-Methoxyphenyl)-1H-pyrazole (Table 2, entry 9)

¹H NMR (CDCl₃, 300 MHz, δ , ppm): 3.77 (s, 3H), 6.36 (t, 1H), 6.89 (d, 2H, $J = 9$ Hz), 7.51 (d, 2H, $J = 9$ Hz), 7.62

(d, 1H, $J = 1.2$ Hz), 7.75 (d, 1H, $J = 2.4$ Hz). ¹³C NMR (75 MHz, CDCl₃, δ , ppm): 55.58, 107.17, 114.51, 120.92, 126.83, 134.04, 140.63, 158.24. MS (EI): m/z (%) 174 [M^+].

3.3.8 | 1-(2-Methyl-4-nitrophenyl)-1H-pyrazole (Table 2, entry 11)

¹H NMR (CDCl₃, 300 MHz, δ , ppm): 2.46 (s, 3H), 6.53 (t, 1H), 7.54 (d, 1H, $J = 8.7$ Hz), 7.73 (d, 1H, $J = 2.4$ Hz), 7.79 (d, 1H, $J = 1.5$ Hz), 8.14 (dd, 1H, $J^1 = 8.7$ Hz, $J^2 = 2.4$ Hz), 8.22 (d, 1H, $J = 2.4$ Hz). ¹³C NMR (75 MHz, CDCl₃, δ , ppm): 19.10, 107.58, 122.02, 126.27, 126.82, 130.50, 134.35, 141.56, 144.67, 146.61. MS (EI): m/z (%) 203 [M^+].

3.3.9 | 1-(4-Bromophenyl)-1H-pyrazole (Table 2, entry 12)

¹H NMR (CDCl₃, 300 MHz, δ , ppm): 6.49 (t, 1H), 7.59 (AB q, 4H), 7.74 (d, 1H, $J = 2.4$ Hz), 7.90 (d, 1H, $J = 2.4$ Hz). ¹³C NMR (75 MHz, CDCl₃, δ , ppm): 108.06, 119.63, 120.58, 126.65, 132.47, 138.41, 141.42. MS (EI): m/z (%) 221 [M^+].

3.3.10 | 1-(4-Methoxyphenyl)-1H-1,2,4-triazole (Table 2, entry 14)

¹H NMR (CDCl₃, 300 MHz, δ , ppm): 3.79 (s, 3H), 6.93 (d, 2H, $J = 8.7$ Hz), 7.50 (d, 2H, $J = 8.7$ Hz), 8.01 (s, 1H), 8.38 (s, 1H). ¹³C NMR (75 MHz, CDCl₃, δ , ppm): 55.64, 114.83, 121.99, 130.47, 152.41, 159.47. MS (EI): m/z (%) 175 [M^+].

3.3.11 | 1-(4-Bromophenyl)-1H-1,2,4-triazole (Table 2, entry 16)

¹H NMR (CDCl₃, 300 MHz, δ , ppm): 7.59 (q, 4H), 8.10 (s, 1H), 8.55 (s, 1H). ¹³C NMR (75 MHz, CDCl₃, δ , ppm): 121.43, 132.86, 135.98, 138.83, 140.80, 152.76. MS (EI): m/z (%) 223 [M^+].

3.3.12 | 1-(4-Methoxyphenyl)-1H-benzo[d][1-3]triazole (Table 2, entry 17)

¹H NMR (CDCl₃, 300 MHz, δ , ppm): 3.93 (s, 3H), 7.14 (d, 2H, $J = 8.4$ Hz), 7.45 (t, 1H), 7.55 (t, 1H), 7.6 (d, 1H, $J = 8.1$ Hz), 8.16 (d, 1H, $J = 8.1$ Hz). ¹³C NMR (75 MHz, CDCl₃, δ , ppm): 55.68, 110.26, 114.98, 120.22, 124.43, 128.03, 130.00, 132.65, 146.32, 159.84. MS (EI): m/z (%) 225 [M^+].

4 | CONCLUSIONS

In summary, we have reported an efficient procedure for the synthesis of Cu nanorods using a polydentate ligand. The application of the Fe₃O₄@SiO₂/EP.EN.EG@Cu catalyst in *N*-arylation of nitrogen-containing heterocycles has been examined, and high yields of the products were achieved. In addition, the catalyst could be easily recovered and reused for at least five cycles.

REFERENCES

- [1] R. Hili, A. K. Yudin, *Nat. Chem. Biol.* **2006**, *2*, 284.
- [2] F. Ullmann, *Ber. Dtsch. Chem. Ges.* **1903**, *36*, 2382.
- [3] I. Goldberg, *Ber. Dtsch. Chem. Ges.* **1906**, *39*, 1691.
- [4] W. Shi, C. Liu, A. Lei, *Chem. Soc. Rev.* **2011**, *40*, 2761.
- [5] N. Rodriguez, L. J. Goossen, *Chem. Soc. Rev.* **2011**, *40*, 5030.
- [6] Y. Yamamoto, *Heterocycles* **2012**, *85*, 799.
- [7] H. He, S. Dong, Y. Chen, Y. Yang, Y. Le, W. Bao, *Tetrahedron* **2012**, *68*, 3112.
- [8] A. B. Sheremetev, N. V. Palysaeva, M. I. Struchkova, K. Y. Suponitsky, M. Y. Antipin, *Eur. J. Org. Chem.* **2012**, 2266.
- [9] Y.-F. Wang, X. Zhu, S. Chiba, *J. Am. Chem. Soc.* **2012**, *134*, 3679.
- [10] Y. Zhang, X. Yang, Q. Yao, D. Ma, *Org. Lett.* **2012**, *14*, 3056.
- [11] K. Jouvin, A. Coste, A. Bayle, F. Legrand, G. Karthikeyan, K. Tadiparthi, G. Evano, *Organometallics* **2012**, *31*, 7933.
- [12] L. A. Bauer, N. S. Birenbaum, G. J. Meyer, *J. Mater. Chem.* **2004**, *14*, 517.
- [13] D. A. Wang, F. Zhou, C. W. Wang, W. M. Liu, *Micropor. Mesopor. Mater.* **2008**, *116*, 658.
- [14] Y. Tai, K. Tajiri, *Appl. Catal. A* **2008**, *342*, 113.
- [15] A. Corma, P. Serna, *Science* **2006**, *313*, 332.
- [16] Y. L. Yang, K. M. Saoud, V. Abdelsayed, G. Glaspell, S. Deevi, M. S. El-Shall, *Catal. Commun.* **2006**, *7*, 281.
- [17] M. Steffan, A. Jakob, P. Claus, H. Lang, *Catal. Commun.* **2009**, *10*, 437.
- [18] G. Vitulli, M. Bernini, S. Bertozzi, E. Pitzalis, P. Salvadori, S. Coluccia, G. Martra, *Chem. Mater.* **2002**, *141*, 183.
- [19] A. A. Athawale, P. P. Katre, M. Kumar, M. B. Majumdar, *Mater. Chem. Phys.* **2005**, *91*, 507.
- [20] Y. Liu, Y. Chu, Y. Zhuo, L. Dong, L. Li, M. Li, *Adv. Funct. Mater.* **2007**, *17*, 933.
- [21] A. Mitra, A. Bhaumik, *Mater. Lett.* **2007**, *61*, 659.
- [22] K. C. Anyaogu, A. V. Fedorov, D. C. Neckers, *Langmuir* **2008**, *24*, 4340.
- [23] D. W. Zhang, T. H. Yi, C. H. Chen, *Nanotechnology* **2005**, *16*, 2338.
- [24] A. K. Patra, A. Dutta, A. Bhaumik, *Catal. Commun.* **2010**, *11*, 651.
- [25] C. J. Xu, J. Xie, D. Ho, C. Wang, N. Kohler, E. G. Walsh, J. R. Morgan, Y. E. Chin, S. H. Sun, *Angew. Chem. Int. Ed.* **2008**, *47*, 173.
- [26] Y. M. Lee, M. A. Garcia, N. A. F. Huls, S. H. Sun, *Angew. Chem. Int. Ed.* **2010**, *49*, 1271.
- [27] W. Li, Y. Deng, Z. Wu, X. Qian, J. Yang, Y. Wang, D. Gu, F. Zhang, B. Tu, D. Zhao, *J. Am. Chem. Soc.* **2011**, *133*, 1583.
- [28] M. Rajabzadeh, H. Eshghi, R. Khalifeh, M. Bakavoli, *RSC Adv.* **2016**, *6*, 19331.
- [29] Z. L. Xu, H. X. Li, Z. G. Ren, W. Y. Du, W. C. Xu, J. P. Lang, *Tetrahedron* **2011**, *67*, 5282.
- [30] L. Xu, D. Zhu, F. Wu, R. Wang, B. Wan, *Tetrahedron* **2005**, *61*, 6553.
- [31] D. Talukdar, G. Das, S. Thakur, N. Karak, A. J. Thakur, *Catal. Commun.* **2015**, *59*, 238.
- [32] F. Heidarizadeh, A. Majdi-nasab, *Tetrahedron Lett.* **2015**, *56*, 6360.

How to cite this article: Rajabzadeh, M., Eshghi, H., Khalifeh, R., and Bakavoli, M. (2016), Magnetically recoverable copper nanorods and their catalytic activity in Ullmann cross-coupling reaction, *Appl. Organometal. Chem.*, doi: 10.1002/aoc.3647